Boundary-Layer Meteorol (2006) 120:437–454
DOI 10.1007/s10546-006-9071-7

ORIGINAL ARTICLE

A parameterization of third-order moments for the dry convective boundary layer

Séverine Tomas · Valéry Masson

Received: 24 May 2005 / Accepted: 6 March 2006 /
Published online: 3 June 2006
© Springer Science+Business Media, Inc. 2006

Abstract We describe one-dimensional (1D) simulations of the countergradient zone of mean potential temperature $\overline{\theta}$ observed in the convective boundary layer (CBL). The method takes into account the third-order moments (TOMs) in a turbulent scheme of relatively low order, using the turbulent kinetic energy equation but without prognostic equations for other second-order moments. The countergradient term is formally linked to the third-order moments $\overline{w'^2\theta'}$ and $\overline{w'\theta'^2}$, and a simple parameterization of these TOMs is proposed. It is validated for several cases of a dry CBL, using large-eddy simulations that have been realized from the MESO-NH model. The analysis of the simulations shows that TOMs are responsible for the inversion of the sign of $\partial\overline{\theta}/\partial z$ in the higher part of the CBL, and budget analysis shows that the main terms responsible for turbulent fluxes and variances are now well reproduced.

Keywords Convective boundary layer · Countergradient term · Heat flux · Parameterization · Third-order moments · Turbulence

1 Introduction

In the convective boundary layer (CBL), the vertical gradient of the mean potential temperature ($\overline{\theta}$) usually takes two forms: unstable in the lower part and slighty stable in the upper part. This means that, in the latter zone, the heat transport is countergradient, and consequently, the eddy-diffusivity formulation of the heat transport, $\overline{w'\theta'} = -K(\partial\overline{\theta}/\partial z)$, is not physically appropriate (Deardorff 1966, 1972; Schumann 1987; Ebert et al. 1989). In order to take into consideration this countergradient transport, and thus to simulate more accurately the dynamics of the CBL, two main approaches can be identified:

– the "mass-flux" parameterization: $\overline{w'\theta'} = M(\theta_u - \overline{\theta})$ where u refers to the strong updraught and M is the mass flux associated with the ensemble of updraughts;
– the Reynolds-average approach, (i) for low-order models: the "eddy-diffusivity" parameterization is used with countergradient term $\overline{w'\theta'} = -K(\partial\overline{\theta}/\partial z - \gamma)$ where K ($\mathrm{m^2\,s^{-1}}$)

S. Tomas (✉) · V. Masson
CNRM/GMME/TURBAU, METEO France, 42, Avenue Gaspard Coriolis, Toulouse, Cedex 01, France
e-mail: Severine.tomas@meteo.fr

is the turbulent diffusivity and γ ($\mathrm{K\,m^{-1}}$) is the countergradient potential temperature gradient, which is the nonlocal term added to the basic eddy-diffusivity formulation in order to take care of the countergradient transport. (ii) For high-order models: nonlocal terms (third-order moments) in the prognostic equations for the second-order moments (SOMs) are used directly.

The "mass-flux" parameterization is related to the studies of cumulus convection that describe the vertical ascent of convective structures and moist convection (Ooyama 1971; Betts 1973; Yanai et al. 1973; Arakawa and Schubert 1974; Betchtold et al. 2001). This mass-flux formulation has also been used to parameterize the transport initiated by thermals in the atmospheric boundary layer (ABL). In order to model the whole range of turbulent transport, Lappen and Randall (2001), after Randall et al. (1992), combined higher-order closure with mass-flux approaches. This step towards unifying parameterizations of cloud and ABL processes is still limited, because this method uses higher-order models that are computationally costly. Siebesma and Teixeira (2000), Teixeira and Siebesma (2000), Soares et al. (2002, 2004) and Hourdin et al. (2002) proposed another way of uniting these parameterizations, by combining both eddy-diffusivity and mass-flux approaches. Cheinet (2003) extended the multiple mass-flux parameterization to surface-generated convection, handling dry convection, moist convection and convective cloudiness in the same framework. However, Cheinet (2003) conceded that his model needed further work, in order to improve the physical description of the downward driven buoyant motions and the overturning process.

Concerning the "eddy-diffusivity" parameterization for low-order models, a constant γ countergradient term of the order of $0.7 \times 10^{-3}\,\mathrm{K\,m^{-1}}$ was first used, which was estimated from the derivation of the heat-flux equation (Deardorff 1966, 1972) and which took into account either buoyancy effects alone, or buoyancy effects combined with transport effects suitably parameterized (Holstag and Moeng 1991). Cuijpers and Holtslag (1998) adopted the same approach, but instead used an integral form of the scalar flux over the whole ABL, while Holtslag and Moeng (1991) used either the surface flux (for bottom-up diffusion) or entrainment flux (for top down-diffusion). Cuijpers and Holtslag (1998) linked the vertical flux to downgradient diffusion, buoyancy and transport effects.

For the higher-order models, the nonlocality of the CBL is taken into account by the TOMs, which are obtained from higher-order closure assumptions. However, this process is computationally heavy as, in a 1D vertical scheme, it needs the resolution of seven prognostic equations:

$$\frac{\partial \overline{u'^2}}{\partial t};\ \frac{\partial \overline{v'^2}}{\partial t};\ \frac{\partial \overline{w'^2}}{\partial t};\ \frac{\partial \overline{u'w'}}{\partial t};\ \frac{\partial \overline{v'w'}}{\partial t} = f\big[\text{mean variables; prognostic SOMs; TOMs}\big],$$

$$\frac{\partial \overline{\theta'^2}}{\partial t} = f\big[\text{mean variables; prognostic SOMs; TOMs}\big],$$

$$\frac{\partial \overline{w'\theta'}}{\partial t} = f\big[\text{ mean variables; prognostic SOMs; TOMs}\big].$$

It is necessary to have a formulation of the TOMs in order to solve these seven partial differential equations since they use TOMs' gradients. For the second-order moment (SOM) models, TOMs are parameterized, but for the third-order models, TOM equations have to be to solved from fourth-order closures.

In a second-order scheme, Mellor and Yamada (1974) parameterized the TOMs with mean gradient terms only, whereas Zeman and Lumley (1976) used buoyancy terms, by coupling the energy flux to the gradients of vertical heat flux and temperature variance, which permitted

a description of the coutergradient transport. Sun and Ogura (1980) modified the Mellor–Yamada formulations so as to incorporate the Zeman–Lumley buoyancy transport closure in their second-order model. Moeng and Wyngaard (1989) evaluated contempory parameterizations for turbulent transport and showed that these formulations did not accurately simulate some turbulence statistics: they suggested a top-down and bottom-up decomposition. Canuto et al. (1994) obtained analytical TOMs, by direct inversion of their prognostic equations that used the quasi-normal approximation for the fourth-order moments (FOMs). This method avoided the use of the clipping approximation (André et al. 1976), which consists of limiting the growth of TOMs when they violate generalized Schwarz inequalities. This still remains computationally costly since it computes prognostically second- and third-order moments. However, this approach reduces the sensitivity of the results of their second-order model to the value of the model constants, and thus, this model proposed by Canuto et al. (1994) is more efficient when it is used to solve more general CBL cases.

Afterwards, Canuto et al. (2001), using a second-order model (prognostic equations for all second order moments), suggested a new analytical expression for the TOMs, simpler and with better physical content, avoiding the quasi-normal approximation for the fourth-order moments and the resulting unphysical growth of the TOMs. Canuto et al. (2005) continued their investigation into the divergence of second-order closure models due to this unrealistic increase of the TOMs. They showed that this divergence is due to the local nature of such models and that it could be canceled out by an appropriate non-local model for TOMs. Suggesting a new closure for the FOMs deduced from aircraft data of several FOM vertical profiles, Cheng et al. (2005) solved the TOM equations and then employed these TOMs in a second-order model. Abdella and McFarlane (1997) and Gryanik and Hartmann (2002) used a mass-flux decomposition for the higher-order terms.

In the present study, we adopt an eddy-diffusivity approach, linking γ to the TOMs by re-solving the Reynolds equations for a 1.5-order turbulent scheme. As developed in Section 2 and in the Appendix A, this 1.5-order model is less complex than a second-order model since, in a 1D vertical scheme, it only requires the resolution of a prognostic equation for the turbulent kinetic energy, e:

$$\frac{\partial e}{\partial t} = f\big[\text{ mean variables; TOMs}\big],$$

with seven diagnostic equations for the other turbulent quantities:

$$\overline{u'^2};\ \overline{v'^2};\ \overline{w'^2};\ \overline{u'w'};\ \overline{v'w'} = f\big[\text{ mean variables } ; e\big],$$
$$\overline{\theta'^2} = f\big[\text{ mean variables; } e\text{; TOMs}\big],$$
$$\overline{w'\theta'} = f\big[\text{ mean variables; } e\text{; TOMs}\big].$$

So, for turbulent quantities, this model is reduced to one differential equation for $\partial e/\partial t$ and seven algebraic equations, in contrast to seven differential equations for the second-order models. Another point of interest in this attempt at computational simplification is that the TOMs are not obtained from higher-order closure assumptions, but from TOMs of a large-eddy simulation (LES) reference case (Section 3). This approach allows us to describe in detail the process of non-local transport, since the countergradient term uses the TOMs that are responsible for this non-local behaviour. The proposed formulation of the countergradient term, which takes TOMs into account, is more computational friendly than a higher-order closure parameterization. A validation of this approach, through a comparison with 1D simulations and LES, both done with the MESONH model, is explained further in Section 4. The main conclusions are afterwards summarized in Section 5.

2 Derivation of the countergradient (CG) terms

The inversion of Reynolds' equations are used to obtain the TOMs and to point out their role in turbulent transport. The goal here is to formally derive the relationship between the TOMs and the countergradient term, in both the heat flux and heat variance equations. The novelty of this work consists in introducing this derivation, because it allows the introduction of TOMs in a 1.5-order scheme.

The evolution equation for the momentum fluxes, the turbulent kinetic energy, the heat flux and the potential temperature variance read, following the Cheng et al. (2002) notations:

$$\frac{\partial}{\partial t}(b_{ij}) + U_k \frac{\partial}{\partial x_k}(b_{ij}) = \underbrace{-\frac{\partial}{\partial x_k}\left(\overline{b'_{ij}u'_k}\right)}_{\text{TR}} \underbrace{-\frac{4}{3}eS_{ij} - \Sigma_{ij} - Z_{ij}}_{\text{DP}} \underbrace{+B_{ij}}_{\text{TP}} \underbrace{-\Pi_{ij}}_{\text{PC}}, \tag{1a}$$

$$\frac{\partial}{\partial t}(e) + U_k \frac{\partial}{\partial x_k}(e) = \underbrace{-\frac{\partial}{\partial x_k}\left(\overline{e'u'_k} + \overline{p'u'_k}\right)}_{\text{TR}} \underbrace{-\overline{u'_k u'_l}\frac{\partial U_k}{\partial x_l}}_{\text{DP}} \underbrace{+\beta_k \overline{u'_k \theta'}}_{\text{TP}} \underbrace{-\epsilon}_{\text{DISS}}, \tag{1b}$$

$$\frac{\partial}{\partial t}(\overline{u'_i\theta'}) + U_k \frac{\partial}{\partial x_k}(\overline{u'_i\theta'}) = \underbrace{-\frac{\partial}{\partial x_k}\left(\overline{u'_k u'_i \theta'}\right)}_{\text{TR}} \underbrace{-\overline{u'_k\theta'}\frac{\partial U_i}{\partial x_k} - \overline{u'_i u'_k}\frac{\partial \overline{\theta}}{\partial x_k}}_{\text{DP}} \underbrace{+\beta_i \overline{\theta'^2}}_{\text{TP}} \underbrace{-\Pi_{i\theta}}_{\text{PC}}, \tag{1c}$$

$$\frac{\partial}{\partial t}(\overline{\theta'^2}) + U_k \frac{\partial}{\partial x_k}(\overline{\theta'^2}) = \underbrace{-\frac{\partial}{\partial x_k}\left(\overline{u'_k\theta'^2}\right)}_{\text{TR}} \underbrace{-2\overline{u'_k\theta'}\frac{\partial \overline{\theta}}{\partial x_k}}_{\text{DP}} \underbrace{-\epsilon_\theta}_{\text{DISS}}, \tag{1d}$$

where $\overline{\theta}$ is the mean potential temperature and θ' the deviation of the potential temperature (θ) from its mean value; hence $\theta' = \theta - \overline{\theta}$. U_i is the mean wind component in the ith direction and u'_i the deviation of the wind component (u_i) from its mean value; $u'_i = u_i - U_i$. The subscript i ranges from 1 to 2 for the horizontal wind components and equals 3 for the vertical component. Overbars indicate Reynolds averaging.

In Eq. (1),

$$b_{ij} = \overline{u'_i u'_j} - \frac{2}{3}\delta_{ij}e, \tag{2a}$$

$$Z_{ij} = R_{ik}b_{kj} - b_{ik}R_{kj}, \tag{2b}$$

$$S_{ij} = \frac{1}{2}\left(\frac{\partial U_i}{\partial x_j} + \frac{\partial U_j}{\partial x_i}\right), \tag{2c}$$

$$R_{ij} = \frac{1}{2}\left(\frac{\partial U_i}{\partial x_j} - \frac{\partial U_j}{\partial x_i}\right), \tag{2d}$$

$$\Sigma_{ij} = b_{ik}S_{kj} + S_{ik}b_{kj} - \frac{2}{3}\delta_{ij}b_{km}S_{mk}, \tag{2e}$$

$$B_{ij} = \beta_i \overline{u'_j\theta'_v} + \beta_j \overline{u'_i\theta'_v} - \frac{2}{3}\delta_{ij}\beta_k \overline{u'_k\theta'_v}. \tag{2f}$$

On the left-hand side of Eq. (1c) for the heat flux and of the potential temperature variance equation (1d), the first term corresponds to the tendency and the second to the advection by

the mean flow. For Eq. (1c), the right-hand side terms are the turbulent transport (TR), the two components of the dynamic production term (DP), the thermal production term (TP) and the pressure correlation term (PC). As for Eq. (1d), terms represent the turbulent transport (TR), the dynamic production term (DP) and the dissipation term (DISS).

The dissipative terms are modelled using the Kolmogorov hypotheses:

$$\epsilon = C_\epsilon \frac{e^{3/2}}{L_\epsilon}, \tag{3a}$$

$$\epsilon_\theta = 2C_{\epsilon_\theta} \frac{\sqrt{e}}{L_\epsilon} \overline{\theta'^2}, \tag{3b}$$

and the pressure correlation terms are estimated as:

$$\Pi_{ij} = C_{pv} \frac{\sqrt{e}}{L} (b_{ij}) - \frac{4}{3}\alpha_0 e S_{ij} - \alpha_1 \Sigma_{ij} - \alpha_2 Z_{ij} + (1-\alpha_3) B_{ij}, \tag{4a}$$

$$\Pi_{i\theta} = C_{p\theta} \frac{\sqrt{e}}{L} (\overline{u_i' \theta'}) - \frac{3}{4}\alpha_4 \left(S_{ij} + \tilde{\alpha_4} R_{ij}\right) \overline{u_j' \theta'} + \alpha_5 \beta_i \overline{\theta' \theta_v'}, \tag{4b}$$

where C_ϵ, C_{pv}, α_0, α_1, α_2, α_3, C_{ϵ_θ}, $C_{p\theta}$, α_4, $\tilde{\alpha_4}$, α_5 are constants given in Table 1.

Redelsperger and Someria (1981) and Cuxart et al. (2000) developed a turbulence scheme suitable for LES and mesoscale configurations with, respectively, a three-dimensional (3D) subgrid-scale and a single-column parameterization. The same assumptions are made here, except that, during the inversion of the system of Eqs. (1a–1d), the TOMs involving temperature are witheld. The extended formulation of these TOMs will be given in the next section. The assumptions used are:

- horizontal homogeneity is assumed (the horizontal gradients of the mean quantities and the vertical gradient of the mean vertical velocity are neglected); this allows the construction of a 1D turbulent scheme for which mean variables only depend on z and t;
- tendency and mean advections are neglected except for the prognostic turbulent kinetic energy. This means that the subgrid turbulent terms are in balance with the gradients of the mean quantities along the border of the mesh;
- nonisotropic terms are suppressed in the equations of heat and water (Redelsperger and Someria 1981) where there are isotropic terms. This hypothesis is quite valid in the mixed part of the ABL, where the turbulence is isotropic. However, this assumption is not valid in the shear layers, such as the surface layer, where the turbulence is clearly nonisotropic. In order to take into account the anisotropic terms when the assumption of isotropy is violated, the subgrid-scale lengths, namely the dissipative and diffusive lengths, near the surface are modified for the dissipation and for the diffusion processes, as shown by Redelsperger et al. (2001).

Table 1 Fixed constants in the turbulent scheme

C_ϵ	C_{pv}	α_0	α_1	α_2	α_3	C_{ϵ_θ}	$C_{p\theta}$	α_4	$\tilde{\alpha_4}$	α_5
0.7	4	0.6	1	1	0	1.2	4	1	1	1/3

After inversion of the linear system (which is developed in the Appendix A), for the 1D dry scheme case, one obtains:

$$\overline{u'w'} = -\frac{4}{15C_{pv}} L\sqrt{e}\frac{\partial U}{\partial z}, \tag{5a}$$

$$\overline{v'w'} = -\frac{4}{15C_{pv}} L\sqrt{e}\frac{\partial V}{\partial z}, \tag{5b}$$

$$\overline{u'^2} = \frac{2}{3}e + \frac{L}{C_{pv}\sqrt{e}}\left\{(1-\alpha_2)\frac{4L\sqrt{e}}{15C_{pv}}\left(\frac{\partial U}{\partial z}\right)^2 - \frac{2}{3}\alpha_3\beta\overline{w'\theta'}\right\}, \tag{5c}$$

$$\overline{v'^2} = \frac{2}{3}e + \frac{L}{C_{pv}\sqrt{e}}\left\{(1-\alpha_2)\frac{4L\sqrt{e}}{15C_{pv}}\left(\frac{\partial V}{\partial z}\right)^2 - \frac{2}{3}\alpha_3\beta\overline{w'\theta'}\right\}, \tag{5d}$$

$$\overline{w'^2} = \frac{2}{3}e + \frac{L}{C_{pv}\sqrt{e}}\left\{-(1-\alpha_2)\frac{4L\sqrt{e}}{15C_{pv}}\left[\left(\frac{\partial U}{\partial z}\right)^2 + \left(\frac{\partial V}{\partial z}\right)^2\right] + \frac{4}{3}\alpha_3\beta\overline{w'\theta'}\right\}, \tag{5e}$$

$$\begin{aligned}\overline{w'\theta'} = &-\frac{2}{3C_{p\theta}} L\sqrt{e}\frac{\partial\overline{\theta}}{\partial z}\,\phi_3 - \frac{2}{3C_{p\theta}} L\sqrt{e}\,\phi_3\frac{\beta}{e}\frac{L_\epsilon}{2C_{\epsilon_\theta}\sqrt{e}}\frac{\partial\overline{w'\theta'^2}}{\partial z}\\ &-\frac{2}{3C_{p\theta}} L\sqrt{e}\,\phi_3\frac{3}{2e}\frac{\partial\overline{w'^2\theta'}}{\partial z},\end{aligned} \tag{5f}$$

$$\begin{aligned}\overline{\theta'^2} = &\,CLL_\epsilon\phi_3\left(\frac{\partial\overline{\theta}}{\partial z}\right)^2 - \phi_3\frac{L_\epsilon}{2C_{\epsilon_\theta}\sqrt{e}}\frac{\partial\overline{w'\theta'^2}}{\partial z}\\ &+ C\phi_3\frac{\partial\overline{\theta}}{\partial z}\frac{3LL_\epsilon}{2e}\frac{\partial\overline{w'^2\theta'}}{\partial z},\end{aligned} \tag{5g}$$

where

$$\phi_3 = \frac{1}{1+CR_\theta}, \tag{6}$$

$$D = [1+CR_\theta]\left[1+\frac{1}{2}CR_\theta\right], \tag{7}$$

$$C = \frac{2}{3C_{p\theta}C_{\epsilon_\theta}}, \tag{8}$$

$$R_\theta = \frac{\beta LL_\epsilon}{e}\frac{\partial\overline{\theta}}{\partial z}. \tag{9}$$

The horizontal wind components, the mean vertical component and its vertical fluctuation are now represented by U, V, W and w'. Outside the surface boundary layer, the mixing and the dissipative lengths are defined according to $L = L_\epsilon = \frac{1}{\sqrt{1/(2.8l_{\rm up})^2+1/(2.8l_{\rm down})^2}}$, with $l_{\rm up}$ and $l_{\rm down}$ as in Bougeault and Lacarrère (1989). In the surface layer where turbulence is anisotropic, these dissipation and diffusion processes are modified following Redelsperger et al. (2001). All constants are the same as in Cuxart et al. (2000) (see also Table 1).

The derivatives of TOMs enter into the formulation of $\overline{\theta'^2}$ and $\overline{w'\theta'}$, and this enables countergradient transport. The turbulent vertical flux of temperature can be expressed as:

$$\overline{w'\theta'} = -K(\partial\overline{\theta}/\partial z - \gamma), \tag{10}$$

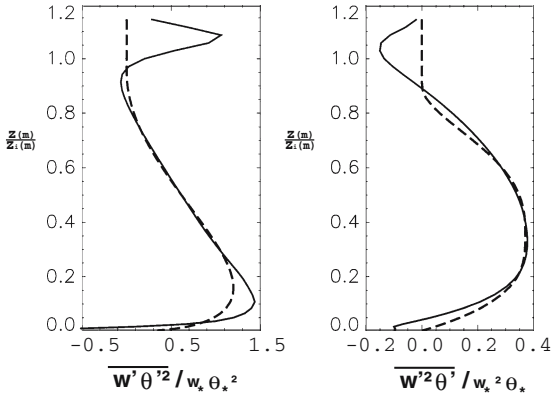

Fig. 1 Normalized TOMs profiles: $\overline{w'\theta'^2}/w_*\theta_*^2$ (left) and $\overline{w'^2\theta'}/w_*^2\theta_*$ (right). The chosen formulation profiles (dashed line) are superposed on the 06F LES ones (solid line)

with

$$K = \frac{2}{3C_{p\theta}} L\sqrt{e}\,\phi_3. \tag{11}$$

The expression for γ is then deduced:

$$\gamma = \frac{\beta}{e}\frac{L_\epsilon}{2C_{\epsilon_\theta}\sqrt{e}}\frac{\partial\overline{w'\theta'^2}}{\partial z} + \frac{3}{2e}\frac{\partial\overline{w'^2\theta'}}{\partial z}. \tag{12}$$

3 Derivation of the third-order moments (TOMs)

The objective of our study is to improve the formulation of the eddy-diffusivity schemes in the countergradient zone of the CBL. Therefore, particular attention will be given to the formulation of the TOMs in that zone, as well as in the unstably stratified zone below. However, because the turbulent scheme must be as general as possible and be valid under different stability conditions, these TOMs must naturally cancel each other out for neutral and stable stratifications. That is why a formulation based on the convective normalization is proposed, such that the convective TOMs terms become weaker as neutrality is approached.

The proposed formulations for TOMs are dimensionless functions of z/z_i, where z_i is the inversion height diagnosed as the minimum heat flux, of w_*, the vertical convective scale, and of θ_* the temperature convective scale. Note that the inversion zone is not treated, because there is no dimensionless universal form for turbulent quantities in this layer. This is due to the complex interactions between additional processes specific to the inversion zone (shear with free atmosphere, gravity waves in the inversion) and turbulent transport of the ABL.

The expressions are established from the statistics of a LES simulation for a convective case (06F, described in Section 4). These formulations, shown in Fig. 1, are:

For $\dfrac{z}{z_i} < 0.9$,

$$\overline{w'^2\theta'} = f\left(w_*\theta_*, \frac{z}{z_i}\right) = \theta_* w_*^2\left[-7.9\left|\frac{z}{z_i} - 0.35\right|^{2.9}\left|\frac{z}{z_i} - 1\right|^{0.58} + 0.37\right], \tag{13}$$

for $\frac{z}{z_i} \geq 0.9$,

$$\overline{w'^2\theta'} = 0,$$

for $\frac{z}{z_i} < 0.95$,

$$\overline{w'\theta'^2} = g\left(w_*\theta_*, \frac{z}{z_i}\right) = \theta_*^2 w_* \left[4\left(\frac{z}{z_i}\right)^{0.4} \left|\frac{z}{z_i} - 0.95\right|^2\right], \tag{14}$$

for $\frac{z}{z_i} \geq 0.95$,

$$\overline{w'\theta'^2} = 0,$$

where $|\ \ |$ represents the absolute value of the quantity. These expressions, even if they are derived for a purely convective case, are not really limited to convective cases. In the neutral and stable ABL, TOMs degenerate because their normalizations are adapted for the CBL. These parameterizations have been tested on the intercomparison case of Nieuwstadt et al. (1993) and on several cases in Ayotte et al. (1995). The simulations have been performed using the MESO-NH model (Lafore et al. 1998), which allows the implementation of these TOMs.

4 Results

4.1 Presentation of the computational tools and simulated cases

4.1.1 LES simulations

In order to validate these parameterizations, several simulations (LES, 1D simulations with and without TOMs) of the dry convective atmosphere have been performed. The 1D simulations with and without TOMs are carried out using the scheme developed in Section 2. The LESs use a 3D turbulent scheme, based on the scheme proposed by Redelperger and Sommeria (1981, 1986) and discussed in detail by Cuxart et al. (2000). It sets up a prognostic equation for subgrid kinetic energy and incorporates the effects of thermal stratification on subgrid fluxes through variable Prandtl and Schmidt numbers. This 3D scheme is able to represent turbulence sources due to shear in all three spatial dimensions. The mixing length is chosen following Deardoff (1974), and is limited both by grid mesh size (supposing layer eddies are resolved explicitly by the 3D model) and by stability.

4.1.2 The dry CBL simulated for validation

The simulated cases of the dry CBL are defined by Ayotte et al. (1995) and Nieuwstadt et al. (1993). The latter, here referred as "06F", was used in the early 1990s, by four groups of LES modellers, for an intercomparison test; "06F" is an example of a dry CBL without a mean wind, and has already been used to test the turbulent scheme of Cuxart et al. (2000). All these simulations have been simulated with the MESO-NH model in a LES configuration, used as a reference, and in a 1D turbulent scheme (with or without TOMs). The LES database of all these validations is provided in Table 2. L_x, L_y, L_z, are the size of the domain in the x, y, z directions; n_x, n_y, n_z, the number of points in the x, y, z directions; Q_* is the surface heat

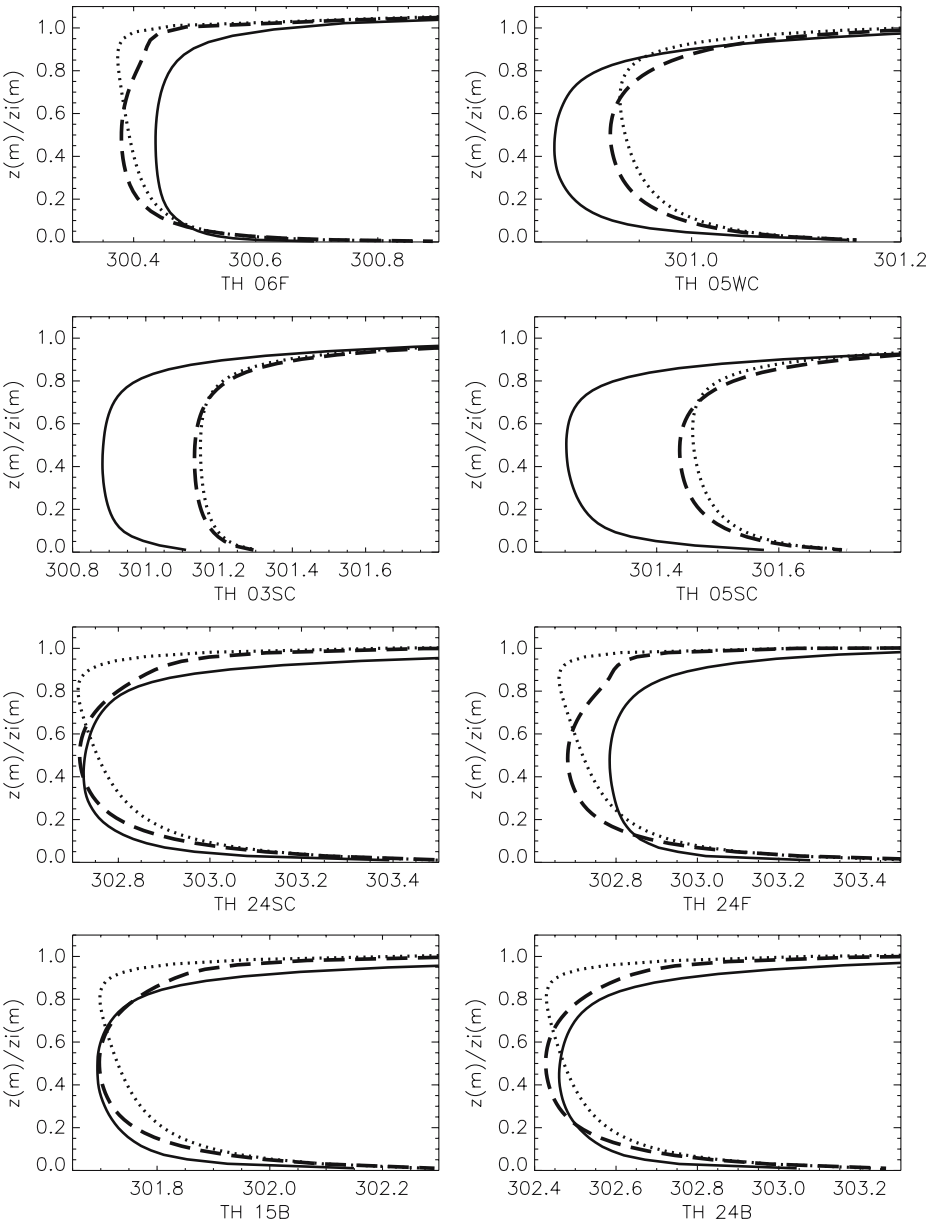

Fig. 2 $\overline{\theta}$ profiles (K) plotted from LES (solid lines), 1D simulations without TOMs (dotted lines) and 1D simulations with TOMs (dashed lines)

flux; U_g, V_g, the geostrophic wind components in the x, y directions; T is the duration of the simulation for each simulation; z_0, the roughness length is fixed at 0.16 m.

4.1.2.1 Free-convection cases In this work, free-convection cases refer to simulations with zero mean wind. For the high surface flux case (24F), a strong capping inversion is

Table 2 Case description (F stands for free convection; WC for weak capping inversion; SC for strong capping inversion and B for baroclinic)

Case	L_x, L_y, L_z (km)	n_x, n_y, n_z	Q_* (K m s^{-1})	U_g(m s^{-1})	V_g(m s^{-1})	T (s)
06F	$16 \times 16 \times 2$	$256 \times 256 \times 45$	0.06	0	0	21600
05WC	$5 \times 5 \times 2$	$96 \times 96 \times 96$	0.05	15	0	13575
03SC	$3 \times 3 \times 1$	$96 \times 96 \times 96$	0.03	15	0	9360
05SC	$3 \times 3 \times 1$	$96 \times 96 \times 96$	0.05	15	0	7740
24SC	$3 \times 3 \times 1$	$96 \times 96 \times 96$	0.24	15	0	7680
24F	$5 \times 5 \times 2$	$96 \times 96 \times 96$	0.24	0	0	7200
15B	$5 \times 5 \times 2$	$96 \times 96 \times 96$	0.15	10	0–20	8640
24B	$5 \times 5 \times 2$	$96 \times 96 \times 96$	0.24	10	0–20	7620

Here L_x, L_y, L_z are the domain sizes in the x, y, z directions; n_x, n_y, n_z are the number of points in the x, y, z directions; Q_* is the surface heat flux; U_g, V_g are the geostrophic wind components in the x, y directions; T is the duration of the simulation for each simulation

imposed at 1000 m, in order to limit the growth of the ABL with time. For the low surface flux case (06F), a weaker capping inversion has been enforced.

4.1.2.2 Buoyancy with shear cases These simulations include various combinations of shear and buoyancy forcing varying from strongly buoyant flows with small shear (run 24SC), to small buoyancy with strong shear (run 03SC). Two capping inversions have been used; strong (03SC, 05SC and 24SC) and weak (05WC).

4.1.2.3 Baroclinic cases Two simulations (runs 15B and 24B) with varying baroclinic forcing, strong capping inversion and different values of surface buoyancy forcing are included. The baroclinic effects are related to geostrophic wind shear.

4.2 Qualitative analysis

4.2.1 Mean potential temperature profiles

In all the simulated cases, the implementation of TOMs improves the 1D simulations. There is not much impact at the scale of the whole ABL and at the inversion level, but the improvement in the mixed layer (Fig. 2) is clear for all cases. With TOMs, the countergradient zone in the upper half of the ABL, where $\overline{\theta}$ increases with height, is correctly simulated by the 1D scheme.

4.2.2 Potential temperature variance profiles

Systematically, the 1D simulations with TOMs give higher values of $\overline{\theta'^2}$ (Fig. 3). On the one hand, for cases with non-zero mean wind (WC, SC, B), the implementation of TOMs improves $\overline{\theta'^2}$; 1D simulations with TOMs give $\overline{\theta'^2}$ profiles closer to the LES than 1D simulations without TOMs. The difference between 1D simulations and LES is greater for low fluxes. On the other hand, for the zero wind 06F and 24F cases, 1D simulations without TOMs produce better $\overline{\theta'^2}$ profiles (closer to LES) than those with TOMs. In those cases, it seems that the implementation of TOMs makes $\overline{\theta'^2}$ rise excessively. However, this occurs in the lower part of the CBL, whereas the main improvement is expected in the upper part

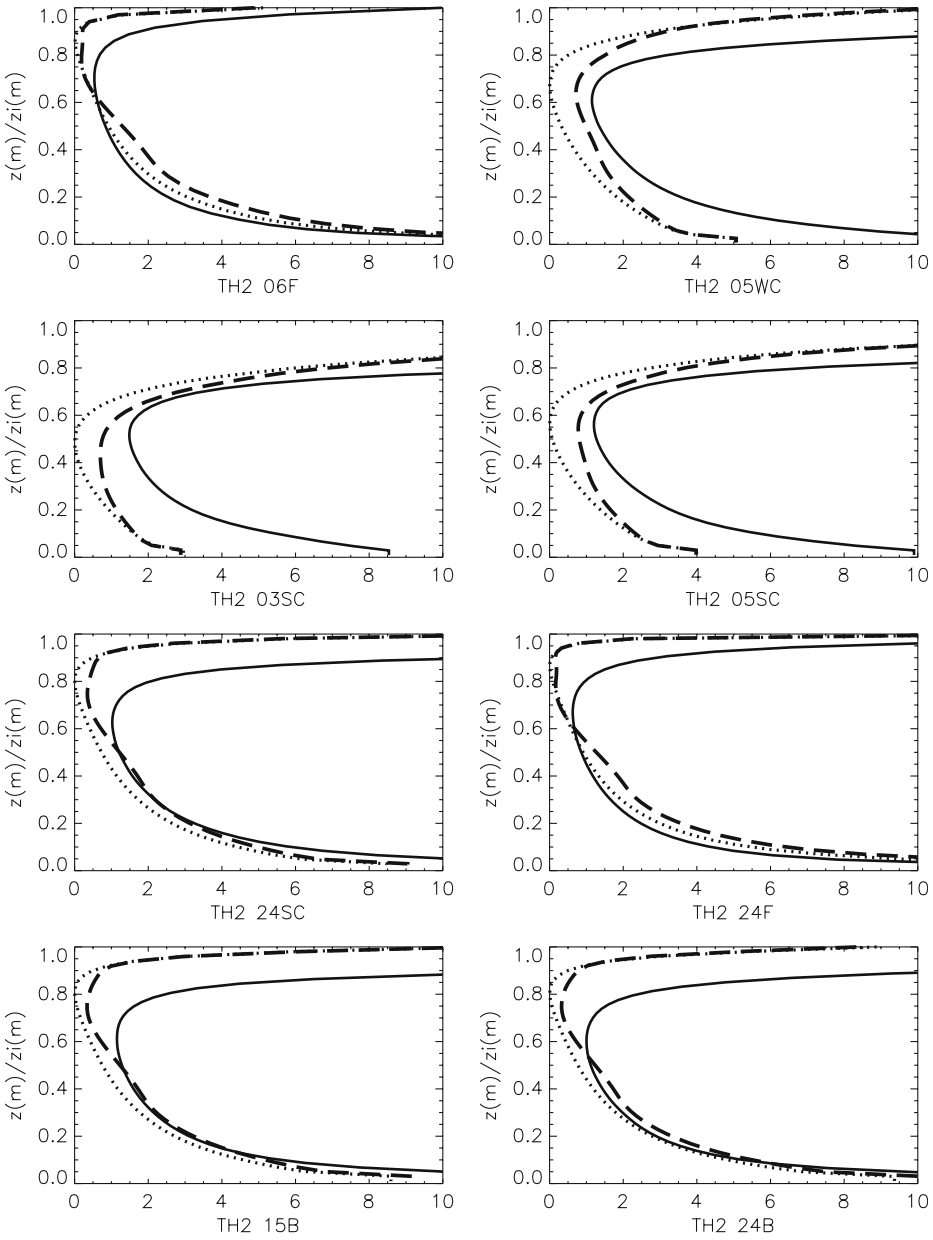

Fig. 3 Normalized variance of $\overline{\theta'^2}/\theta_*^2$ plotted from LES (solide lines), 1D simulations without TOMs (dotted lines) and 1D simulations with TOMs (dashed lines)

of the CBL, where the countergradient zone is observed. Finally, a general tendency can be observed in the mixed layer, the use of TOMs decreases the underestimated temperature variance, and thus improves the simulation of the countergradient zone. Futhermore, all 1D simulations underestimate $\overline{\theta'^2}$ in the inversion layer. However, this common tendency cannot

be improved with the analytical TOMs, since their formulations are valid for z/z_i lower than 0.9. For all cases, the temperature variance never reaches zero for 1D simulations with TOMs. On the contrary, $\overline{\theta'^2}$ reaches zero in the mixed layer for simulations without TOMs. This is not physical and due to the fact that for the eddy-diffusivity parameterization without the TOMs, $\overline{\theta'^2}$ is proportional to $\left(\partial\overline{\theta}/\partial z\right)^2$.

4.3 Analyses of vertical profiles of heat flux and potential temperature variance budgets

The improvement of the physics of the creation/destruction processes of temperature variance and heat flux is now studied. The detailed budget equation for $\overline{\theta'^2}$ and $\overline{w'\theta'}$ is shown in Fig. 4 for case 24F. The behaviour of each term is the same for all of the other cases simulated and described above. For $\overline{\theta'^2}$ and $\overline{w'\theta'}$ budgets, if TOMs are not taken into account, there is no transport term. Then, the dissipative term is balanced only by the dynamic production term for $\overline{\theta'^2}$ budget and an equilibrium is reached between the pressure correlation term and the dynamic production term associated with the temperature flux production term in the $\overline{w'\theta'}$ budget. When TOMs are implemented (simulations with TOMs), a transport term appears in the budget. With TOMs, the new balances obtained are then closer to the LES budget terms. These profiles indicate how TOMs improve the 1D simulations. Indeed, since the turbulent transport is introduced by TOMs, the implementation of the TOMs in the turbulence scheme allows a countergradient zone in the $\overline{\theta}$ profile for the upper part of the ABL (see Fig. 2), which initiates the negative zone of dynamic production for the $\overline{\theta'^2}$ and $\overline{w'\theta'}$ profiles. As noted, the TOMs parameterizations do not extend into the inversion zone, and we do not expect improvement in this layer.

4.4 Statistical analysis

Each 1D simulation with or without TOMs is now compared to the LES statistics, the latter encompassing the sum of resolved and subgrid processes. As our TOMs parameterizations are not applicable in the inversion layer, the data presented in Table 3 correspond to the mixed layer only.

In bold are indicated relative improvements of more than 10% between 1D simulations. Thanks to the countergradient terms from TOMs, the normalized vertical gradient of temperature, $\partial\overline{\theta}/\partial z$, is systematically improved with TOMs, which is encouraging, since the main goal of the TOMs implementation is to improve the simulation of the thermal turbulent transport. However, the effects of the TOMs implementation on the normalized heat flux, $\overline{w'\theta'}$, are less marked: the surface and the inversion fluxes control the behaviour of $\overline{w'\theta'}$, which shows almost a linear decrease (in z) between the surface flux and the inversion flux. Between 1D without TOMs and 1D with TOMs, those surface and inversion fluxes are unchanged. So, there is no significant discrepancy between the profile of $\overline{w'\theta'}$ with or without TOMs. As the turbulent kinetic energy production (shear and $\beta\overline{w'\theta'}$) and destruction terms (using L_ε) are not significantly modified, there is almost no impact on turbulent kinetic energy. On the contrary, for the variance, $\overline{\theta'^2}$, the standard deviation and the bias are generally improved with the TOMs, which was to be expected, since the aim of our study was to formulate and to implement TOMs in the expression of $\overline{\theta'^2}$, so as to improve CBL simulations.

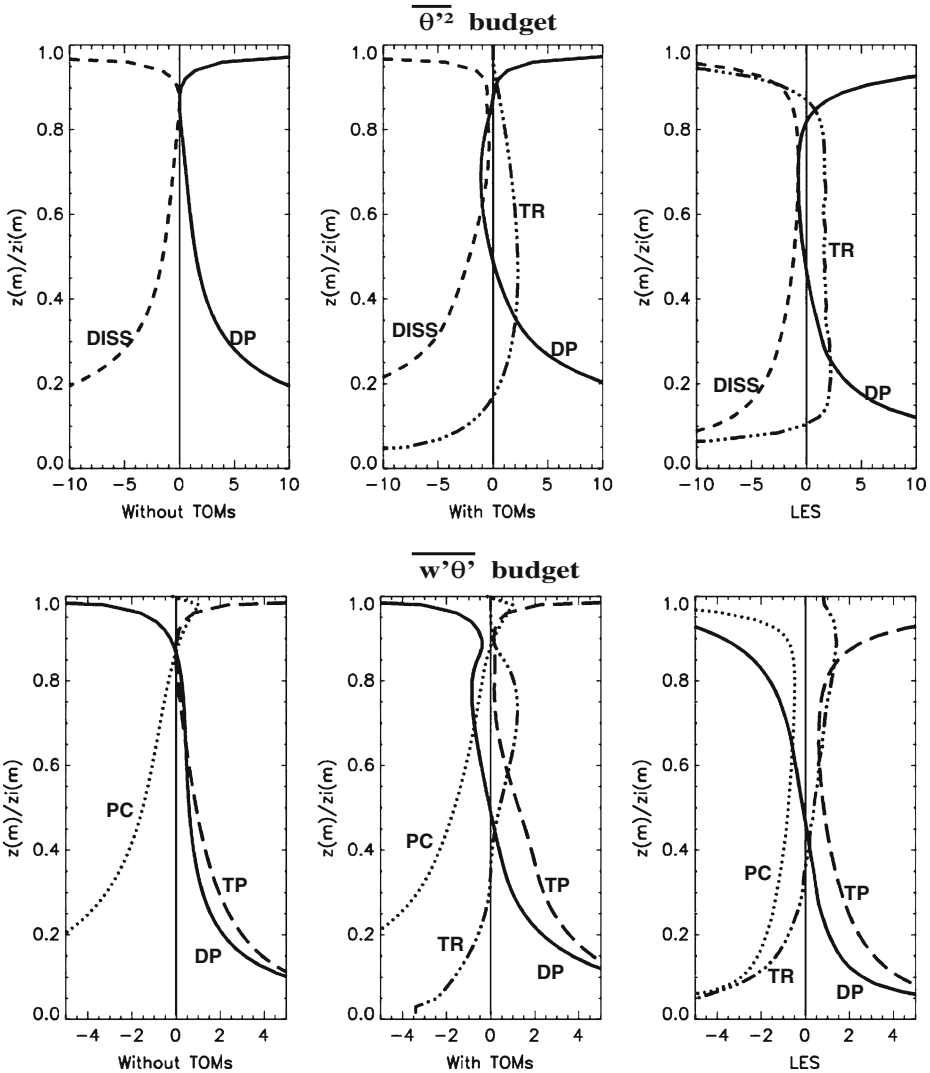

Fig. 4 Contributions of the normalized dynamic production term (DP), the dissipative term (DISS) and the turbulent transport term (TR) for $\overline{\theta'^2}$ (higher part) and the dynamic production term (DP), the temperature flux production term (TP), the pressure correlation term (PC) and the turbulent transport term (TR) for $\overline{w'\theta'}$ (lower part) for the 24F case

5 Conclusions

In order to represent the countergradient zone of $\overline{\theta}$, third-order moments (TOMs) for temperature flux and for variance have been incorporated in the 1.5-order scheme of Cuxart et al. (2000). In a dry CBL case, the resultant expressions for the variance, $\overline{\theta'^2}$, and heat flux, $\overline{w'\theta'}$, incorporate two additional terms that contain $\overline{w'^2\theta'}$ and $\overline{w'\theta'^2}$. The link between TOMs and the countergradient term is:

Table 3 Comparison of simulations without TOMs ("no TOMs") to LES and simulations with TOMs ("TOMs") to LES (F stand for free convection; WC for weak capping inversion; SC for strong capping inversion, and B for baroclinic). TKE is the turbulent kinetic energy

		$\overline{\theta}/\theta_*$		$\frac{\partial\overline{\theta}}{\partial z}/\left(\frac{\theta_*}{z_i}\right)$		$\overline{w'\theta'}/w_*\theta_*$		$\overline{\theta'^2}/\theta_*^2$		TKE / w_*^2	
		SD	bias	SD	bias	SD	bias	SD	bias	SD	bias
06F	no TOMs	0.0289	−0.0165	0.0175	−0.0601	0.0077	0.0057	**0.3492**	**0.0298**	0.0918	**0.0570**
	TOMs	**0.0126**	**−0.0092**	**0.0148**	**−0.0286**	**0.0062**	**0.0045**	0.4438	0.1788	0.1068	0.0715
05WC	no TOMs	0.0436	0.0267	0.0068	−0.0168	0.0378	−0.0222	0.9600	−0.5689	0.1475	0.0824
	TOMs	**0.0354**	0.0220	**0.0031**	**−0.0084**	**0.0329**	**−0.0195**	**0.6641**	**−0.3395**	0.1486	0.0829
03SC	no TOMs	0.1459	0.0815	0.0102	−0.0166	0.1439	−0.0756	1.3578	−0.6811	0.1392	0.0662
	TOMs	0.1388	0.0776	**0.0067**	**0.0092**	0.1362	−0.0716	**0.9882**	**−0.4585**	0.1398	0.0664
05SC	no TOMs	0.1153	0.0644	0.0071	−0.0110	0.1005	−0.0530	0.9014	−0.4866	0.1253	0.0655
	TOMs	0.1049	0.0586	**0.0030**	**−0.0023**	0.0923	−0.0488	**0.5475**	**−0.2705**	0.1263	0.0660
24SC	no TOMs	0.0505	0.0051	0.0241	−0.0324	0.0081	−0.0045	0.7813	−0.3712	0.1052	0.0430
	TOMs	**0.0179**	**−0.0002**	**0.0157**	**−0.0160**	**0.0042**	**−0.0025**	**0.6233**	**−0.2001**	0.1069	0.0444
24F	no TOMs	0.0650	**−0.0287**	0.0191	−0.0292	0.0157	0.0090	**0.3272**	**−0.0199**	0.1493	0.0881
	TOMs	**0.0549**	−0.0332	**0.0135**	**−0.0131**	0.0169	0.0095	0.4834	0.1055	0.1498	0.0884
15B	no TOMs	0.0478	0.0036	0.0330	−0.0311	0.0061	−0.0018	1.6050	−0.5629	0.0700	0.0132
	TOMs	**0.0187**	**0.0008**	**0.0278**	**−0.0193**	**0.0035**	**0.0008**	1.5050	**−0.3960**	0.0720	0.0141
24B	no TOMs	0.0546	**−0.0058**	0.0357	−0.0575	**0.0014**	**−0.0001**	1.0071	−0.3637	0.0923	0.0350
	TOMs	**0.0254**	−0.0117	**0.0223**	**−0.0275**	0.0051	0.0027	**0.9046**	**−0.1936**	0.0950	0.0362

$$\gamma = \frac{\beta}{e}\frac{L_\epsilon}{2C_{\epsilon_\theta}\sqrt{e}}\frac{\partial\overline{w'\theta'^2}}{\partial z} + \frac{3}{2e}\frac{\partial\overline{w'^2\theta'}}{\partial z},$$

where $\beta = g/\overline{\theta}$, e is the turbulent kinetic energy, C_{ϵ_θ} is the constant in the $\overline{\theta'^2}$ dissipation and L_ϵ is the dissipative length.

A parameterization of the TOMs has been proposed, and the validation compares LES, 1D simulation without TOMs and 1D simulation with TOMs to several cases of dry CBL already documented (Cuxart et al. 2000; Ayotte et al. 1995). These simulations cover different states of the atmosphere: free convective, buoyant with wind shear, baroclinic, with strong or weak capping inversion, and with various surface flux forcings. The analysis of these simulations reveals that, as has been shown statistically by comparisons with LES, the implementation of TOMs generally improves 1D simulations. Indeed, the countergradient zone for $\overline{\theta}$ is then predicted and the budgets of variance, $\overline{\theta'^2}$, and of heat flux, $\overline{w'\theta'}$, actually contain a turbulent transport term, which was lacking in the initial version of the 1D model. More precisely, the analysis of the stationary budgets of $\overline{w'\theta'}$ and $\overline{\theta'^2}$ shows a much better physical partitioning between dynamical production, turbulent transport (TOMs), and pressure correlation or dissipation. The new formulation produces a negative dynamical production in the countergradient zone.

However, this formulation does not permit a description of the inversion layer and it is yet to be tested for moist convection. This generalization will be another step in the parameterization of TOMs.

Acknowledgements The study is supported by the MesoScale Meteorology group of the National Center of Meteorological Research. The authors would like to thank Joel Stein and Jean-Luc Redelsperger for providing

us with helpful comments and Pierre Lacarrère and Joel Noilhan for fruitful discussions. Special thanks to Jean Maziejewski for valuable comments and suggestions.

Appendix A

The inversion of the system (1a)–(1d) is developed. Applying the hypotheses of Section 2, the linear system to be inverted is:

$$0 = -(1-\alpha_2)\frac{\partial U}{\partial z}b_{13} - \frac{2}{3}\alpha_3\beta\overline{w'\theta'} - C_{pv}\frac{\sqrt{e}}{L}b_{11}, \tag{A1}$$

$$0 = -(1-\alpha_2)\frac{\partial V}{\partial z}b_{23} - \frac{2}{3}\alpha_3\beta\overline{w'\theta'} - C_{pv}\frac{\sqrt{e}}{L}b_{22}, \tag{A2}$$

$$0 = +(1-\alpha_2)\frac{\partial U}{\partial z}b_{13} + (1-\alpha_2)\frac{\partial V}{\partial z}b_{23} + \frac{4}{3}\alpha_3\beta\overline{w'\theta'} - C_{pv}\frac{\sqrt{e}}{L}b_{33}, \tag{A3}$$

$$0 = b_{12}, \tag{A4}$$

$$0 = -\frac{4}{15}e\frac{\partial U}{\partial z} - C_{pv}\frac{\sqrt{e}}{L}b_{13}, \tag{A5}$$

$$0 = -\frac{4}{15}e\frac{\partial V}{\partial z} - C_{pv}\frac{\sqrt{e}}{L}b_{23}, \tag{A6}$$

$$0 = \overline{u'\theta'}, \tag{A7}$$

$$0 = \overline{v'\theta'}, \tag{A8}$$

$$0 = -\frac{\partial\overline{w'^2\theta'}}{\partial z} - \frac{2}{3}e\frac{\partial\overline{\theta}}{\partial z} + \frac{2}{3}\beta\overline{\theta'^2} - C_{p\theta}\frac{\sqrt{e}}{L}\overline{w'\theta'}, \tag{A9}$$

$$0 = -\frac{\partial\overline{w'\theta'^2}}{\partial z} - 2\frac{\partial\overline{\theta}}{\partial z}\overline{w'\theta'} - 2C_{\epsilon_\theta}\frac{\sqrt{e}}{L_\epsilon}\overline{\theta'^2}, \tag{A10}$$

where

$$b_{11} = \overline{u'^2} - \frac{2}{3}e, \tag{A11}$$

$$b_{22} = \overline{v'^2} - \frac{2}{3}e, \tag{A12}$$

$$b_{33} = \overline{w'^2} - \frac{2}{3}e, \tag{A13}$$

$$b_{23} = \overline{v'w'}, \tag{A14}$$

$$b_{12} = \overline{u'v'}, \tag{A15}$$

$$b_{13} = \overline{u'w'}. \tag{A16}$$

By substitution, one obtains:

$$\overline{u'w'} = -\frac{4}{15C_{pv}}L\sqrt{e}\frac{\partial U}{\partial z}, \tag{A17}$$

$$\overline{v'w'} = -\frac{4}{15C_{pv}}L\sqrt{e}\frac{\partial V}{\partial z}, \tag{A18}$$

$$\overline{u'^2} = \frac{2}{3}e + \frac{L}{C_{pv}\sqrt{e}}\left\{+(1-\alpha_2)\frac{4L\sqrt{e}}{15C_{pv}}\left(\frac{\partial U}{\partial z}\right)^2 - \frac{2}{3}\alpha_3\beta\overline{w'\theta'}\right\}, \tag{A19}$$

$$\overline{v'^2} = \frac{2}{3}e + \frac{L}{C_{pv}\sqrt{e}}\left\{+(1-\alpha_2)\frac{4L\sqrt{e}}{15C_{pv}}\left(\frac{\partial V}{\partial z}\right)^2 - \frac{2}{3}\alpha_3\beta\overline{w'\theta'}\right\}, \tag{A20}$$

$$\overline{w'^2} = \frac{2}{3}e + \frac{L}{C_{pv}\sqrt{e}}\left\{-\frac{8}{15}e\frac{\partial W}{\partial z} - (1-\alpha_2)\frac{4L\sqrt{e}}{15C_{pv}}\left[+(\frac{\partial U}{\partial z})^2 + (\frac{\partial V}{\partial z})^2\right] + \frac{4}{3}\alpha_3\beta\overline{w'\theta'}\right\}, \tag{A21}$$

$$\overline{w'\theta'} = -\frac{L}{C_{p\theta}\sqrt{e}}\left[\frac{\partial\overline{w'^2\theta'}}{\partial z} + \frac{2}{3}e\frac{\partial\overline{\theta}}{\partial z} - \frac{2}{3}\beta\overline{\theta'^2}\right], \tag{A22}$$

$$0 = \left\{-\frac{\partial\overline{w'\theta'^2}}{\partial z} + \frac{2L}{C_{p\theta}\sqrt{e}}\frac{\partial\overline{\theta}}{\partial z}\frac{\partial\overline{w'^2\theta'}}{\partial z}F_{w\theta}\right\} + \frac{4L\sqrt{e}}{3C_{p\theta}}\left(\frac{\partial\overline{\theta}}{\partial z}\right)^2 - \left[\frac{4}{3}\frac{L\beta}{C_{p\theta}\sqrt{e}}\frac{\partial\overline{\theta}}{\partial z} + 2C_{\epsilon_\theta}\frac{\sqrt{e}}{L_\epsilon}\right]\overline{\theta'^2}. \tag{A23}$$

Thus, the variance of potential temperature can be extracted,

$$\overline{\theta'^2} = CLL_\epsilon\phi_3\left(\frac{\partial\overline{\theta}}{\partial z}\right)^2 - \phi_3\frac{L_\epsilon}{2C_{\epsilon_\theta}\sqrt{e}}\frac{\partial\overline{w'\theta'^2}}{\partial z} + C\phi_3\frac{\partial\overline{\theta}}{\partial z}\frac{3LL_\epsilon}{2e}\frac{\partial\overline{w'^2\theta'}}{\partial z}, \tag{A24}$$

where

$$\phi_3 = \frac{1}{1+CR_\theta}, \tag{A25}$$

$$D = [1+CR_\theta]\ [1+\frac{1}{2}CR_\theta], \tag{A26}$$

$$C = \frac{2}{3C_{p\theta}C_{\epsilon_\theta}}, \tag{A27}$$

$$R_\theta = \frac{\beta LL_\epsilon}{e}\frac{\partial\overline{\theta}}{\partial z}. \tag{A28}$$

It is then deduced:

$$\overline{w'\theta'} = -\frac{2}{3C_{p\theta}}L\sqrt{e}\frac{\partial\overline{\theta}}{\partial z}\phi_3 - \frac{2}{3C_{p\theta}}L\sqrt{e}\,\phi_3\frac{\beta}{e}\frac{L_\epsilon}{2C_{\epsilon_\theta}\sqrt{e}}\frac{\partial\overline{w'\theta'^2}}{\partial z} - \frac{2}{3C_{p\theta}}L\sqrt{e}\,\phi_3\frac{3}{2e}\frac{\partial\overline{w'^2\theta'}}{\partial z}, \tag{A29}$$

and the 1D dry scheme composed of Eqs. (5a)–(5g) is obtained.

References

Abdella K, McFarlane N (1997) A new second-order turbulence closure scheme for the planetary boundary layer. J Atmos Sci 54:1850–1867

André JC, De Moor G, Lacarrere P, Du Vachat R (1976) Turbulence approximation for inhomogeneous flows. Part 1: the clipping approxiation. J Atmos Sci 33:476–481
Arakawa A, Schubert WH (1974) Interaction of a cumulus cloud ensemble with the largescale environment. Part I. J Atmos Sci 31:674–701
Ayotte KW, et al (1995) An evaluation of neutral and convective planetary boundary-layer parametrizations relative to large eddy simulations. Boundary-Layer Meteorol 79:131–175
Bechtold P, Bazile E, Guichard F, Mascard P, Richard E (2001) A mass flux convection scheme for regional and global models. Quart J Roy Meteorol Soc 127:869–886
Betts AK (1973) Non-precipitating cumulus convection and its parameterization. Quart J Roy Meteorol Soc 32:178–196
Bougeault P, Lacarrère P (1989) Parameterization of orography-induced turbulence in a meso-beta scale model. Mon Wea Rev 117:1870–1888
Canuto VM, Minotti F, Ronchi C, Ypma RM, Zeman O (1994) Second order closure PBL Model with new third-order moments: Comparison with LES datas. J Atmos Sci 51:1605–1618
Canuto VM, Cheng Y, Howard A (2001) New third-order moments for the convective boundary layer. J Atmos Sci 58:1169–1172
Canuto VM, Cheng Y, Howard A (2005) What causes the divergences in local second order closure models? J Atmos Sci 62:1645–1651
Cheinet S (2003) A multiple mass-flux parameterization for the surface-generated convection. J Atmos Sci 60:2313–2327
Cheng Y, Canuto VM, Howard AM (2002) An improved model for the turbulent PBL. J Atmos Sci 59:1550–1565
Cheng Y, Canuto VM, Howard AM (2005) Nonlocal convective PBL model based on new third and fourth order moments. J Atmos Sci 62:2189–2204
Cuijpers JWM, Holtslag AAM (1998) Impact of skewness and nonlocal effects on scalar and buoyancy fluxes in convective boundary layers. J Atmos Sci 55:151–162
Cuxart J, Bougeault P, Redelsperger JL (2000) A turbulence scheme allowing for mesoscale and large-eddy simulations. Quart J Roy Meteorol Soc 126:1–30
Deardorff JW (1966) The counter-gradient heat flux in the lower atmosphere and in the laboratory. J Atmos Sci 23:503–506
Deardorff JW (1972) Numerical investigation of neutral and unstable planetary boundary layer. J Atmos Sci 29:91–115
Deardorff JW (1974) Three-dimensional numerical study of turbulence in an entraining mixed layer. Boundary-Layer Meteorol 7:199–226
Ebert EE, Schumann U, Stull RB (1989) Non local turbulent mixing in the convective boundary layer evaluated from large eddy simulation. J Atmos Sci 46:2178–2207
Gryanik VM, Hartmann J (2002) A turbulence closure for the convective boundary layer based on a two-scale mass-flux approach. J Atmos Sci 59:2729–2744
Hourdin F, Couvreux F, Menut L (2002) Parameterization of the dry convective boundary layer based on a mass-flux representation of thermals. J Atmos Sci 59:1105–1123
Lafore JP, Stein J, Asencio N, Bougeault P, Ducrocq V, Duron J, Fisher C, Hereil P, Mascart P, Masson V, Pinty JP, Redelsperger JL, Richard E, Vila-Guerau de Arellano J (1998) The Meso-NH Atmospheric simulation system. Part I: adiabatic formulation and control simulations. Ann Geophys 16:90–109
Lappen C-L, Randall DA (2001) Toward a unified parameterization of the boundary layer and moist convection. Part I: A new type of mass-flux model. J Atmos Sci 58:2021–2036
Mellor GL, Yamada T (1974) A hierarchy of turbulence closure models for planetary boundary layers. J Atmos Sci 31:1791–1806
Moeng CH, Wyngaard JC (1989) Evaluation of turbulent transport and dissipation closures in second-order modeling. J Atmos Sci 46:2311–2330
Nieuwstadt FTM, Mason PJ, Moeng CH, Schumann U (1993) Large-Eddy simulation of the convective boundary layer: a comparaison of four computer codes. Turbulent Shear Flow Vol. 8, Springer-Verlag, Berlin, pp. 343–367
Ooyama K (1971) A theory on parameterization of cumulus convection. J Meteorol Soc Jpn 49:744–756
Randall DA, Shao Q, Moeng C-H (1992) A second-order bulk boundary layer model. J Atmos Sci 49:1903–1923
Redelsperger JL, Sommeria G (1981) Méthode de représentation de la turbulence d'échelle inférieure à la maille pour un modèle tri-dimensionnel de convection nuageuse. Boundary-Layer Meteorol. 21:509–530
Redelsperger JL, Sommeria G (1986) Three-dimensional simulation of a convective storm: sensitivity studies on subgrid parameterization and spatial resolution. J Atmos Sci 43:2619–2635
Redelsperger JL, Mahé F, Carlotti P (2001) A simple and general subgrid model suitable both for surface layer and free-stream turbulence. Boundary-Layer Meteorol 101:375–408

Schumann U (1987) The counter-gradient heat flux in turbulent stratified flows. Nuclear Engineering and Design 100:255–262
Siebesma AP, Teixeira J (2000) An advection-diffusion scheme for the convective boundary layer, description and 1D results, 14th Symposium on Boundary Layer and Turbulence, Aspen, USA, pp. 133–136
Soares PMM, Miranda P, Siebesma AP, Teixeira J (2002) An advection-diffusion parameterisation turbulence scheme based on TKE equation, 3rd Portuguese-Spanish Assembly of Geodesy and Geophysics, Valencia, Spain, vol. II, pp. 856–859
Soares PMM, Miranda P, Siebesma AP, Teixeira J (2004) An eddy-diffusivity/mass-flux parametrization for dry and shallow cumulus convection. Quart J Roy Meteorol Soc 128:1–18
Sun WY, Ogura Y (1980) Modeling the evolution of the convective planetary boundary layer. J Atmos Sci 37:1558–1572
Teixeira J, Siebesma AP (2000) A mass-flux/K-diffusion approach for the parametrization of the convective boundary layer: global model results, 14th Symp. on Boundary Layer and Turbulence, Aspen, USA, pp. 231–234
Yanai M, Esbensen S, Chu J (1973) Determination of bulk properties of tropical cloud clusters from large-scale heat and moisture budgets. J Atmos Sci 30:611–627
Zeman O, Lumley JL (1976) Modeling buoyancy driven mixed layers. J Atmos Sci 33:1974–1988